

TRANSMISSION ELECTRON MICROSCOPY STUDY OF THE POROUS STRUCTURE OF ALUMINAS SYNTHESIZED BY NON-IONIC SURFACTANT TEMPLATING ROUTE

Isabel DÍAZ¹, Verónica GONZÁLEZ-PEÑA², Carlos MÁRQUEZ-ALVAREZ^{3,*} and Joaquín PÉREZ-PARIENTE⁴

Instituto de Catálisis y Petroleoquímica, CSIC, C/Marie Curie, s/n Cantoblanco, 28049 Madrid, Spain; e-mail: ¹ i.diaz@icp.csic.es, ² vgpena@imp.mx, ³ c.marquez@icp.csic.es, ⁴ jperez@icp.csic.es

Received June 30, 2003

Accepted July 29, 2003

Organized mesoporous and microporous aluminas have been synthesized by a sol-gel route in non-aqueous media using poly(oxyethylene) block polymers as directing agents. Gel compositions adjusted to obtain direct micelles (in 1,4-dioxane solution) and reverse micelles (in cyclohexane solution) were tested. The influence of synthesis conditions, such as temperature, solvent, use of additives or chemical modification of the precursor, on the alumina porous structure has been analysed by transmission electron microscopy (TEM). Mesoporous aluminas with a pore structure originated by the cross-linking of corrugated oxide-hydroxide platelets of nanometric size were obtained using aluminum *sec*-butoxide as precursor. The addition of ammonium fluoride or amines to the synthesis gel, as well as higher calcination temperatures, caused a decrease in the surface area due to the condensation of the crystallites into a dense porous structure composed of small polycrystalline agglomerates. Microporous aluminas with higher density and a disordered but isotropic porous structure were obtained by chemical modification of the alkoxide precursor with chelating agents such as ethyl acetoacetate or triethanolamine.

Keywords: Transmission electron microscopy; Mesostructured alumina; Sol-gel processes; Non-ionic surfactants; Poly(oxyethylene) block polymers; Reverse micelles; Mesoporous materials.

High surface area aluminas are commonly used in industry as catalysts, catalyst supports and adsorbents¹. The improvement of the performance properties of these materials, which strongly depend on their porosity, will therefore have an important economical impact. For this reason, the production of aluminas with a narrow pore size distribution has a great industrial interest, as the performance of classical aluminas is limited by their uncontrolled porosity.

The successful synthesis of silica and aluminosilicates of the M41S family has derived a number of studies on the synthesis of mesostructured aluminas in aqueous²⁻⁹ and non-aqueous media¹⁰⁻¹⁷. As recently reviewed by Čejka¹⁸, reports on the activity of catalysts based on aluminas synthesized by several of these surfactant-assisted routes have been published for a limited number of reactions, including the selective hydrogenation of cinnamaldehyde¹⁹, hydrodesulfurization of thiophene^{20,21}, metathesis of olefins²² and n-hexane hydroisomerization¹⁶, showing in some cases significant improvements in respect to catalysts using conventional aluminas as supports.

The surfactants used to assist the synthesis of these aluminas include anionic (alkylphosphates², alkylsulfonates², dodecylsulfate^{3-6,9}, carboxylic acids⁹⁻¹¹), cationic (hexadecyltrimethylammonium⁷⁻⁹) and non-ionic surfactants (*N,N*-dimethyldodecylamine-*N*-oxide⁹, alkylene oxide block polymers^{9,12-17}). Among the synthesis procedures leading to thermally stable aluminas, the hydrolysis of an aluminum alkoxide in an organic solvent, in the presence of non-ionic surfactants, namely poly(oxyethylene) block polymers (POE)¹², provided the highest surface areas reported for aluminas calcined at temperatures above 500 °C. The addition of small amounts of Ce³⁺ or La³⁺ has been shown to improve the thermal stability of these mesostructured aluminas¹⁴. We have also proved that the addition of amines results in an increased thermal stability of aluminas synthesized by hydrolysis of aluminum *sec*-butoxide in butan-2-ol, in the presence of a POE^{15,16}. Moreover, we have reported that the addition of chelating ligands leads to a dramatic change of both aluminum coordination and pore structure of the porous alumina. Microporous solids with high concentration of tetra- and pentacoordinated aluminum were obtained when the aluminum alkoxide precursor was modified with ethyl acetoacetate or triethanolamine¹⁷.

Besides nitrogen adsorption/desorption data, that evidence the mesoporous or microporous nature of these aluminas, the structural characterization is frequently based on X-ray diffraction data. In general, a single peak at low angle can be distinguished in the reported X-ray diffraction patterns, whose intensity and broadness change as a function of the synthesis conditions. Such a broad reflection is commonly observed in a wide variety of disordered mesoporous solids but also in materials with a very small crystal size. Due to this lack of structural information from X-ray diffraction data, we have carried out a study by transmission electron microscopy (TEM) to give further insights into the pore architecture of micro- and mesoporous aluminas prepared by a non-ionic surfactant-assisted route.

EXPERIMENTAL

The syntheses of mesostructured aluminas were carried out by hydrolysis of aluminum *sec*-butoxide (97%; Acros), using a H₂O:Al ratio of 2, in the presence of a poly(oxyethylene) block polymer, in an organic solvent: butan-2-ol (99.5%; Sigma), 1,4-dioxane (99%; Panreac) or cyclohexane (Panreac). POE surfactants containing different number of oxyethylene (OE) units were used: Triton X-45 and X-114 (4-(1,1,3,3-tetramethylbutyl)phenyl-polyethylene glycol, with 5 and 7–8 OE units, respectively) and Tergitol 15-S-9 and 15-S-15 (containing 9 and 15 OE units, respectively, and a linear alkyl chain with 11 to 15 carbon atoms) were provided by Sigma. The amounts of solvent used were 18.20, 19.46 and 3.2–6.9 mol of butan-2-ol, dioxane and cyclohexane, respectively, per mol of alkoxide. In some syntheses, ammonium fluoride (98%; Aldrich) or an amine (*N,N*-dipropylamine, 99%; 1-propylamine, 98%; 1-hexylamine, 99%; 1-decylamine, 99%; 1-dodecylamine, 98%; or 1-hexadecylamine, 90%; all provided by Aldrich) were added in an additive/alkoxide molar ratio of 0.1–0.25. Other samples were prepared from aluminum *sec*-butoxide chemically modified with ethyl acetoacetate (99%; Aldrich) or triethanolamine (98%; Aldrich), using modifier/alkoxide molar ratios of 0.5 and 0.1, respectively. The chemical modification of the alkoxide was performed prior to the hydrolysis by adding the modifier to the alkoxide solution and stirring the solution at room temperature for 30 min.

In a typical synthesis, the aluminum precursor and the surfactant (in a molar ratio of 10:1), and the amine when used, were dissolved in part of the organic solvent. For the synthesis in reverse micelles systems, the solution was prepared using cyclohexane as solvent and aluminum precursor/surfactant molar ratios of 1 to 2 (ref.²³). The hydrolysis was carried out at room temperature by slowly adding, under stirring, a mixture of water (and the amine or ammonium fluoride when used) and the remaining solvent. The resulting mixture was stirred at room temperature for 3 h, and then kept at room temperature or 95 °C for 24 h. After that, the resulting gelatinous product was filtered, washed with ethanol and dried at 40 °C for 2 days. When the ageing was carried out at room temperature, the dried gel was subsequently heated at 95 °C for 6 h in an open polypropylene bottle. The surfactant was then removed by Soxhlet extraction with ethanol for 15 h. The extracted solid was dried at 40 °C for 2 days and then calcined in a stream of air at 550 °C for 4 h. Some samples were further calcined in an oven at temperatures from 600 to 850 °C for 3 h.

Nitrogen adsorption–desorption isotherms recorded at –196 °C were obtained in an ASAP 2000 Micromeritics apparatus. The samples were evacuated at 350 °C for 24 h prior to the analysis. X-Ray powder diffraction patterns were collected using CuK α radiation, using a Seiffert XRD 3000P diffractometer with a curved graphite secondary monochromator, a primary automatic divergence slit and a 0.2 mm detector slit.

For the TEM experiments, the samples were crushed on an agate mortar, dispersed in acetone and dropped on a holey carbon microgrid. Micrographs were recorded using a JEOL JEM 2000FX microscope operating at 200 kV equipped with an X-ray detector (XEDS) and a Philips 120 Biotwin microscope operating at 120 kV equipped with a Gatan CCD camera.

RESULTS AND DISCUSSION

The synthesized micro- and mesoporous aluminas were calcined at different temperatures in order to study their stability and structure modifications,

and their topotactic transformation to γ - and δ -Al₂O₃ (ref.²⁴). Figure 1 shows nitrogen adsorption–desorption isotherms and X-ray diffractograms of selected micro- and mesoporous samples calcined at 550 °C. The mesoporous aluminas exhibit a single peak at low 2θ values in the X-ray diffraction patterns corresponding to a large d spacing, whose intensity, position and broadness change as a function of the synthesis conditions. This disordered mesostructure is in agreement with the N₂ adsorption/desorption data that correspond to type IV isotherms, showing a well-defined step at relative pressure around 0.5 to 0.8 (ref.¹⁶). For some mesostructured aluminas synthesized in the presence of poly(oxyalkylene) block polymers, previously reported in the literature, the combination of X-ray diffraction and N₂ adsorption/desorption results have been interpreted in terms of “wormlike” channel motif based on the analysis of TEM images^{12,14}. However, our TEM study shows that these X-ray patterns and N₂ isotherms results could be related to a wide variety of porous structures, as it will be discussed below.

Figure 2 (top) shows a TEM image of a sample synthesized in butan-2-ol at 25 °C in the presence of Triton X-114 and calcined at 550 °C, which possesses BET surface area $S_{\text{BET}} = 520 \text{ m}^2/\text{g}$, mean pore diameter $d_p = 5.0 \text{ nm}$

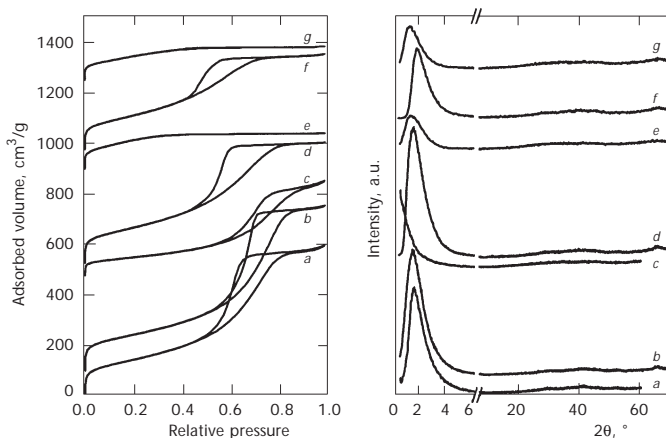


FIG. 1

Nitrogen adsorption–desorption isotherms (left) and X-ray diffractograms (right) of some representative micro- and mesoporous aluminas calcined at 550 °C. Synthesis in butan-2-ol at 25 °C, using Triton X-114 (a); synthesis as in a with addition of 0.1 mol of 1-hexylamine per mol of aluminum (b); synthesis as in a with addition of 0.25 mol of ammonium fluoride per mol of aluminum (c); synthesis in 1,4-dioxane at 95 °C, using Tergitol 15-S-15 (d); synthesis as in d using ethyl acetoacetate-modified aluminum alkoxide (e); synthesis in cyclohexane (0.5 mol per mol of aluminum) at 25 °C, using Triton X-45 (f); synthesis as in f using triethanolamine-modified aluminum alkoxide (g). Data have been incremented for clarity

and pore volume $v_p = 0.88 \text{ cm}^3/\text{g}$, as determined from the nitrogen adsorption-desorption isotherm. No discernible ordering of pores can be distinguished in the TEM image, and the material appears to be built up of very tiny corrugated platelets, which resemble the crystal habit reported for pseudoboehmite^{1,25}. At higher magnification (Fig. 2, bottom), what seems to be the edge of individual platelets can be identified, with an estimated thickness of 2 nm, which corresponds approximately to the packing of three individual boehmite-like layers, each one having a thickness of half of the b parameter of the unit cell of boehmite. It can be concluded from these images that the pore structure is most probably the result of the cross-linking of the crystallites.

The addition of alkyl amines to the synthesis gel modifies the surface area and pore size, and increases the thermal stability of the mesoporous alumina¹⁵. The structure of the stable modified alumina depends on the calcination temperature. Thus, in a sample synthesized in butan-2-ol at 25 °C in the presence of Triton X-114 and *N,N*-dipropylamine (amine/aluminum molar ratio of 0.25) calcined at 550 °C, the already mentioned corrugated platelets are observed, while further calcination at 700 °C leads to a stable

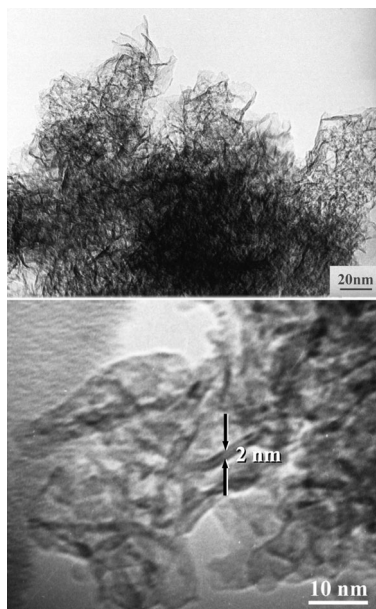


FIG. 2

TEM images of alumina samples synthesized in butan-2-ol, in the presence of Triton X-114. The gel was aged at 25 °C and the obtained solid calcined at 550 °C

material formed by small polycrystalline agglomerates (Fig. 3a), which evidences a partial condensation of the boehmite-like layers. Due to this condensation, the BET surface area and pore volume decrease from 520 to 230 m²/g and from 0.72 to 0.60 cm³/g, respectively, while the mean pore size increases from 4.6 to 8.0 nm. It is worth to mention at this point that the topotactic transformation of boehmite to γ -Al₂O₃ usually occurs at temperatures below 500 °C, and further transformation to δ -Al₂O₃ and α -Al₂O₃ takes place at 700 and 1200 °C, respectively. In marked contrast, the evolution of the polycrystalline material upon calcination at temperatures up to 850 °C (Fig. 3b), followed by X-ray and electron diffraction, allows us to observe the early stages of a retarded transformation into γ -Al₂O₃. X-Ray dif-

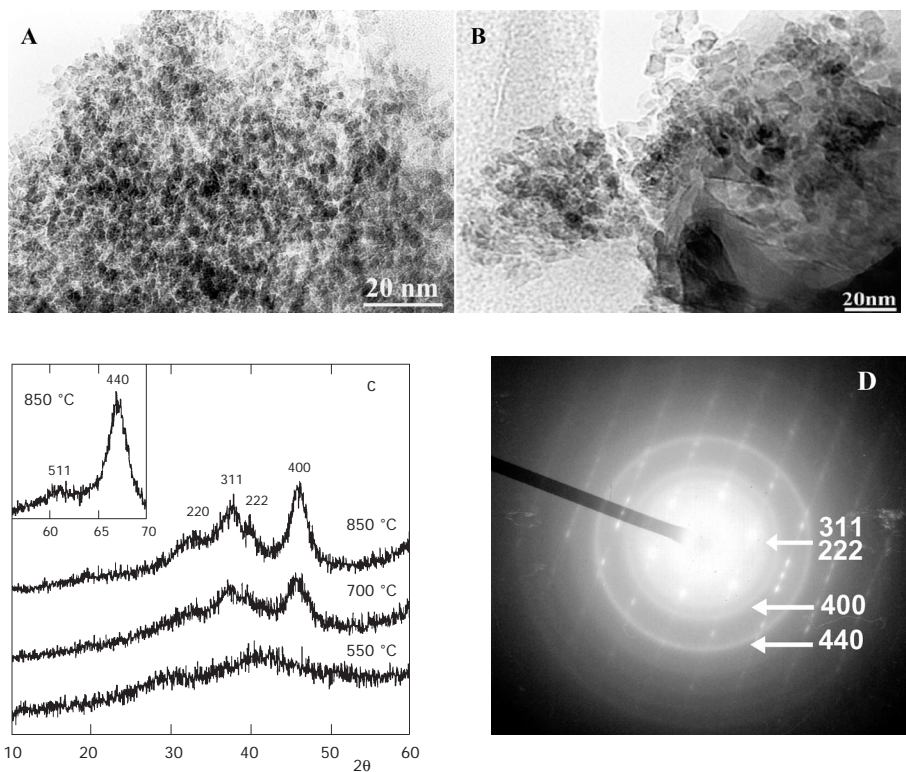


FIG. 3

TEM images of alumina samples synthesized in butan-2-ol, in the presence of Triton X-114 and 0.25 mol of *N,N*-dipropylamine per mol of aluminum. The gel was aged at 25 °C and the obtained solid was calcined at 700 °C (a) and 850 °C (b). X-Ray diffraction patterns of the sample calcined at 550, 700 and 850 °C (c) and electron diffraction pattern of the sample calcined at 850 °C (d)

fraction patterns shown in Fig. 3c demonstrate the appearance of traces of $\gamma\text{-Al}_2\text{O}_3$ in the sample calcined at 700 °C. The reflections corresponding to this phase become intense at 850 °C. The topotactic transformation into $\gamma\text{-Al}_2\text{O}_3$ and further into $\delta\text{-Al}_2\text{O}_3$ is easily evidenced in the electron diffraction pattern of the sample calcined at 850 °C, shown in Fig. 3d. Intense rings due to 400 and 440 reflections as well as diffuse 311 and 222 ones, characteristic of $\gamma\text{-Al}_2\text{O}_3$, are observed in the pattern. On the other hand, the presence of extra triple spots, related to the triple cell parameter of the tetragonal superstructure of $\delta\text{-Al}_2\text{O}_3$, indicate the incipient and delayed transformation from $\gamma\text{-Al}_2\text{O}_3$ to $\delta\text{-Al}_2\text{O}_3$. These data reveal an enhanced thermal stability of these mesostructured aluminas, which results in a higher surface area of the samples calcined at elevated temperature. Several n-alkyl amines of different chain length were also used as additives¹⁶. Among the synthesis conditions and amines tested, hexylamine rendered aluminas with the highest surface area after calcination at 600 °C, higher than 400 m²/g. Interestingly, Čejka *et al.*²⁶ have reported that organized mesoporous aluminas synthesized in the presence of carboxylic acids and calcined at 450 to 1000 °C, are composed of agglomerated crystalline particles showing a structure similar to that in Figs 3a and 3b, although $\delta\text{-Al}_2\text{O}_3$ is detected in the X-ray diffractograms at calcination temperatures from 600 °C.

In order to obtain more acidic aluminas, it would be necessary to increase the number of coordinatively unsaturated Al. For this reason, we have tested the effect of fluoride ions added to the synthesis gel as ammonium fluoride¹⁷. The N₂ adsorption-desorption isotherms of aluminas synthesized in the presence of ammonium fluoride and calcined at 550 °C are characteristic of mesoporous solids. However, even though the hysteresis loop is shifted to higher relative pressure, indicating larger pore size, the materials have smaller BET surface area than those obtained in the absence of fluoride. For example, the addition of 0.25 mol of ammonium fluoride per mol of aluminum in a synthesis gel containing Triton X-114 and aged at room temperature, decreased the surface area to 260 m²/g for the alumina calcined at 550 °C, while the pore volume decreased to 0.56 cm³/g and the pore size increased to 6.8 nm. The explanation could come from the closed packed agglomerate-type structure observed by TEM (Fig. 4). The alumina calcined at 550 °C consists mainly of agglomerated particles formed by very small densely packed platelets, showing a structure similar to that observed in the samples synthesized in the presence of amines and calcined at higher temperatures, and also similar to the TEM images presented in ref.²⁰

In our previous studies, no correlation was observed between pore diameter and surfactant head volume when the synthesis was carried out in butan-2-ol. One plausible explanation for this result is that the surfactant molecules do not form micelles in butan-2-ol under the conditions used in these experiments. In fact, the results reported by Ray²⁷ suggest that the non-ionic surfactants used in these syntheses would not form micelles in alkanol solutions. Therefore, aiming to control the alumina pore size by means of the adequate selection of the surfactant size, we have carried out the synthesis in 1,4-dioxane¹⁷, as POE surfactants form micelles in this solvent²⁸. Furthermore, we have explored the synthesis of porous alumina in reverse micelle systems formed by poly(oxyethylene) block polymers in cyclohexane²³. These studies have shown that when the synthesis is carried out in 1,4-dioxane, the pore size of the alumina increases with the surfactant head volume, which was attributed to the aggregation of the surfactants into micelles. However, the use of direct (1,4-dioxane solution) or reverse (cyclohexane solution) micellar systems has no significant effect on the structure of the alumina. The mesoporous aluminas prepared using either solvent exhibit an intricate cross-linking of corrugated oxide-hydroxide platelets (Figs 5a and 6a), similar to that of the aluminas synthesized in butan-2-ol. Moreover, the BET surface areas are comparable to that of samples prepared from sols obtained in butan-2-ol. Surface areas around 500 m²/g are obtained for samples calcined at 550 °C, and around 350 m²/g for samples calcined at 600 °C.

We have also reported a synthesis route aiming to tailor both aluminum coordination and pore structure of the alumina. This strategy is based on the chemical modification of the aluminum alkoxide precursor with chelat-

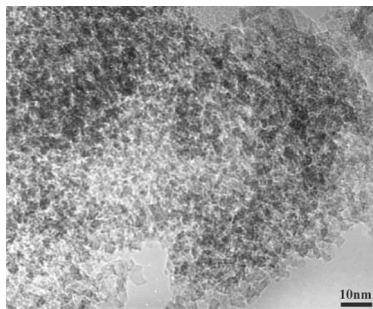


FIG. 4

TEM image of an alumina sample synthesized in butan-2-ol, in the presence of Triton X-114 and 0.25 mol of ammonium fluoride per mol of aluminum. The gel was aged at 25 °C and the obtained solid calcined at 550 °C

ing ligands, in order to retard the hydrolysis and condensation reaction rates²⁹. For this purpose, we have carried out the hydrolysis of aluminum *sec*-butoxide modified with ethyl acetoacetate and triethanolamine. The N₂ adsorption–desorption isotherms of aluminas synthesized with chelating agents either in 1,4-dioxane or cyclohexane and calcined at 550 °C show that these samples are microporous. The TEM image of a sample synthesized from ethyl acetoacetate-modified aluminum *sec*-butoxide in dioxane and calcined at 550 °C (Fig. 5b) shows the presence of irregularly shaped pore channels, in marked contrast to samples synthesized with the non-modified alkoxide in the same solvent. Therefore, the chemical modification of the precursor with ethyl acetoacetate produces a dramatic change in the porous structure of the alumina. Furthermore, the analysis by ²⁷Al MAS NMR spectroscopy showed that such a chemical modification of the precur-

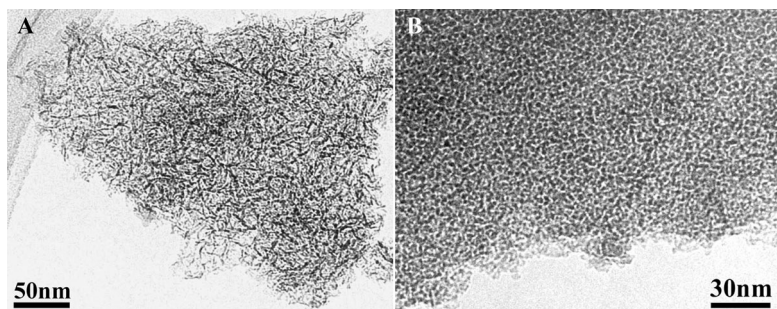


FIG. 5

TEM images of alumina samples synthesized in 1,4-dioxane, in the presence of Tergitol 15-S-15, using no modifier (a) and using ethyl acetoacetate as a modifier (b). The gels were aged at 95 °C and the obtained solids calcined at 550 °C

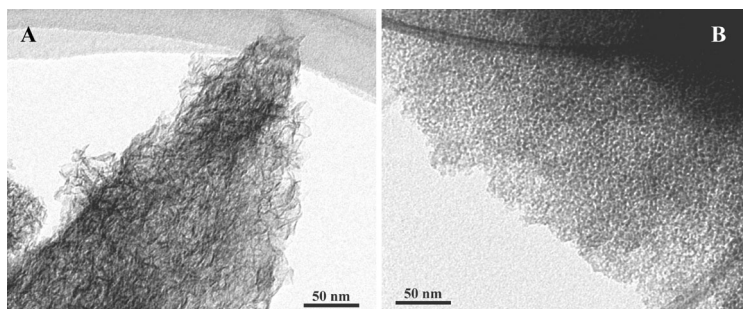


FIG. 6

TEM images of alumina samples synthesized in cyclohexane (0.5 mol per mol of aluminum), in the presence of Triton X-45, using no modifier (a) and using triethanolamine as a modifier (b). The gels were aged at 25 °C and the obtained solids calcined at 550 °C

sor results in an increased number of coordinatively unsaturated aluminum¹⁷. These results suggest that the stability of the chelate with regard to hydrolysis and condensation reactions prevents the formation of the octahedral hydroxyaquo Al(III) complexes that account for the tendency to form the pseudoboehmite platelets in the absence of modifiers. However, it has to be stressed that this change in the porous structure decreases significantly the surface area from 510 m²/g for the mesoporous sample to 310 m²/g for the sample obtained with the ethyl acetoacetate-modified alkoxide, which possesses a micropore volume of 0.11 cm³/g. Using the same approach in reverse micellar system, *i.e.* at higher surfactant content in cyclohexane solution, the obtained triethanolamine-modified aluminum materials result in the same structural change (Fig. 6b) for all the surfactants and synthesis conditions tested²³.

The same trend is observed when modifiers are added to the synthesis gel in butan-2-ol. Both triethanolamine and ethyl acetoacetate produce a denser and isotropic structure (Fig. 7) in sharp contrast with the corrugated platelets observed in the materials prepared without chelating agents (Fig. 2). The lower surface area of the aluminas assesses this increased density. Thus, for a sample synthesized in butan-2-ol at 95 °C in the presence of Triton X-114 and 0.5 mol of ethyl acetoacetate per mol of alumina, calcined at 550 °C, a BET surface area of 325 m²/g was obtained, while the surface area was 510 m²/g when no modifier was used. Slightly denser aluminas were obtained by chemical modification of the alkoxide with triethanolamine, according to the smaller BET surface area (280 m²/g) shown by the sample synthesized adding 0.1 mol of triethanolamine per mol of aluminum.

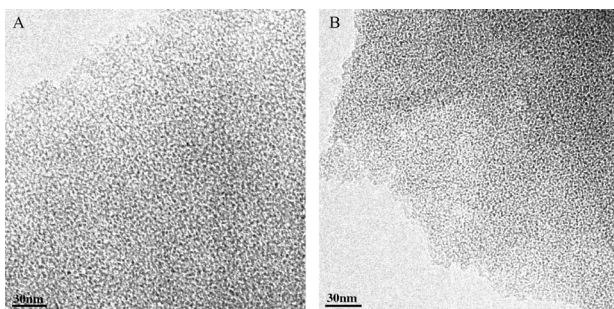


FIG. 7

TEM images of materials synthesized in butan-2-ol, in the presence of Triton X-114, using triethanolamine (a) and ethyl acetoacetate as a modifier (b). The gels were aged at 25 and 95 °C, respectively, and the obtained solids calcined at 550 °C

CONCLUSIONS

This TEM study shows that organized mesoporous aluminas, obtained by hydrolysis of aluminum tri-*sec*-butoxide, in the presence of poly(oxyethylene) block polymers, either in butan-2-ol, 1,4-dioxane or cyclohexane solution, appear to be built up of corrugated platelets of nanometric size. The pore structure of these materials is the result of the cross-linking of the crystallites. The addition of ammonium fluoride or amines, as well as higher calcination temperatures, cause a decrease in the surface area due to the condensation of the aluminum oxide-hydroxide crystallites into a dense porous structure composed of small polycrystalline agglomerates. Microporous aluminas with higher density and a disordered but isotropic porous structure are obtained when chelating agents such as ethyl acetoacetate or triethanolamine are present in the synthesis gel.

This work has been supported by the Spanish CICYT (Project MAT2000-1167-C02-02). The authors thank Centro de Microscopía Electrónica Luis Brú (Universidad Complutense de Madrid, Spain) and Prof. V. Alfredsson (Lund University, Sweden) for providing access to TEM facilities. V. González-Peña thanks CONACyT (México) for the Ph.D. grant.

REFERENCES

1. Misra C.: *Industrial Alumina Chemicals*. ACS Monograph 184. ACS, Washington 1986.
2. Huo Q., Margolese D. I., Ciesla U., Demuth D. G., Feng P., Gier T. E., Sieger P., Firouzi A., Chmelka B. F., Schüth F., Stucky G. L.: *Chem. Mater.* **1994**, *6*, 1176.
3. Yada M., Machida M., Kijima T.: *Chem. Commun.* **1996**, 769.
4. Yada M., Hiyoshi H., Ohe K., Machida M., Kijima T.: *Inorg. Chem.* **1997**, *36*, 5565.
5. Yada M., Kitamura H., Machida M., Kijima T.: *Langmuir* **1997**, *13*, 5252.
6. Yada M., Ohya M., Machida M., Kijima T.: *Chem. Commun.* **1998**, 1941.
7. Cabrera S., El Haskouri J., Alamo J., Beltrán A., Beltrán D., Mendioroz S., Marcos M. D., Amorós P.: *Adv. Mater.* **1999**, *11*, 379.
8. Cabrera S., El Haskouri J., Guillem C., Latorre J., Beltrán-Porter A., Beltrán-Porter D., Marcos M. D., Amorós P.: *Solid State Sci.* **2000**, *2*, 405.
9. Valange S., Guth J.-L., Kolenda F., Lacombe S., Gabelica Z.: *Microporous Mesoporous Mater.* **2000**, *35–36*, 597.
10. Vaudry F., Khodabandeh S., Davis M. E.: *Chem. Mater.* **1996**, *8*, 1451.
11. Čejka J., Žilková N., Rathouský J., Zukal A.: *Phys. Chem. Chem. Phys.* **2001**, *3*, 5076.
12. Bagshaw S. A., Pinnavaia T. J.: *Angew. Chem., Int. Ed. Engl.* **1996**, *35*, 1102.
13. Yang P., Zhao D., Margolese D. I., Chmelka B. F., Stucky G. D.: *Nature* **1998**, *396*, 152.
14. Zhang W., Pinnavaia T. J.: *Chem. Commun.* **1998**, 1185.
15. González-Peña V., Díaz I., Márquez-Alvarez C., Sastre E., Pérez-Pariente J.: *Microporous Mesoporous Mater.* **2001**, *44–45*, 203.
16. González-Peña V., Márquez-Alvarez C., Sastre E., Pérez-Pariente J.: *Stud. Surf. Sci. Catal.* **2001**, *135*, 1072.

17. González-Peña V., Márquez-Alvarez C., Sastre E., Pérez-Pariente J.: *Stud. Surf. Sci. Catal.* **2002**, 142, 1283.
18. Čejka J.: *Applied Catalysis, A: Special Issue "Catalysis by Mesoporous Materials"* **2003**, in press.
19. Valange S., Barrault J., Derouault A., Gabelica Z.: *Microporous Mesoporous Mater.* **2001**, 44–45, 211.
20. Kaluža L., Zdražil M., Žilková N., Čejka J.: *Catal. Commun.* **2002**, 3, 151.
21. Čejka J., Žilková N., Kaluža L., Zdražil M.: *Stud. Surf. Sci. Catal.* **2002**, 141, 243.
22. Onaka M., Oikawa T.: *Chem. Lett.* **2002**, 850.
23. González-Peña V.: *Ph.D. Thesis*. Universidad Autónoma de Madrid, Madrid 2003.
24. Díaz I., González-Peña V., Márquez-Alvarez C., Sastre E., Pérez-Pariente J.: *Zeolites and Microporous Crystals 2000. Proc. Int. Symp., Sendai, August 6, 2000*, p. 200.
25. Ono T., Ohguchi Y., Togari O.: *Stud. Surf. Sci. Catal.* **1983**, 16, 631.
26. Čejka J., Kooyman P. J., Veselá L., Rathouský J., Zúkal A.: *Phys. Chem. Chem. Phys.* **2002**, 4, 4823.
27. Ray A.: *Nature* **1971**, 231, 313.
28. a) Schick M. J., Gilbert A. H.: *J. Colloid Sci.* **1965**, 20, 464; b) Becher P.: *J. Colloid Sci.* **1965**, 20, 728.
29. Brinker C. J., Scherer G. W.: *Sol-Gel Science*. Academic Press, San Diego 1990.